Received: 5 July 2020 | Revised: 22 November 2020 | Accepted: 13 December 2020

DOI: 10.1002/hyp.14014

RESEARCH ARTICLE

WILEY

Hydrologic variability in black ash wetlands: Implications for vulnerability to emerald ash borer

Thomas R. Cianciolo[1] | Jacob S. Diamond[2,3] | Daniel L. McLaughlin[4] | Robert A. Slesak[5] | Anthony W. D'Amato[6] | Brian J. Palik[7]

[1]Department of Forest Resources, University of Minnesota, St. Paul, MN

[2]Quantitative Ecohydrology Laboratory, RiverLy, Irstea, Lyon, France

[3]Continental Geo-hydrosystems Laboratory, University of Tours, Tours, France

[4]Department of Forest Resources and Environmental Conservation, Virginia Tech, Blacksburg, VA

[5]USDA Forest Service, Pacific Northwest Research Station, Olympia, WA

[6]Rubenstein School of Environment and Natural Resources, University of Vermont, Burlington, VT

[7]USDA Forest Service, Northern Research Station, Grand Rapids, MN

Correspondence
Thomas R. Cianciolo, Department of Forest Resources, University of Minnesota, St. Paul, MN, USA
Email: thomrc6@vt.edu

Funding information
Department of Interior Northeast Climate Adaptation Science Center; Minnesota Environmental and Natural Resources Trust Fund; Minnesota Forest Resources Council; USDA Forest Service Northern Research Station

Abstract

Black ash (*Fraxinus nigra*) wetlands are widespread, forested landscape features in the western Great Lakes region. However, the future of these ecosystems is threatened due to impending spread of the invasive emerald ash borer (EAB), which results in tree mortality, decreased transpiration, and potential shifts to wetter, non-forested conditions. The vulnerability to such ecohydrologic shifts likely varies according to local hydrologic regimes controlled by landscape settings, but this site-dependent vulnerability and our ability to predict it is unknown. Here, we assessed vulnerability potential as a function of site hydrology in 15 undisturbed black ash wetlands from their three most common hydrogeomorphic settings in northern Minnesota: lowland, depression, and transition. Further, we used high-resolution (1-cm) surface elevation models to assess spatial variability of water levels at a subset of 10 sites. Although we observed similar ET and groundwater exchange rates among settings, lowland sites were generally drier because of elevated landscape position and greater water level drawdowns (via lower specific yield). We predict that such drier sites will exhibit greater water level increases following EAB-induced ash mortality, compared to wetter sites where open water evaporation and shallow-rooted understory transpiration will offset losses in tree transpiration. Moreover, compared to wetter sites, drier sites exhibited minimal microtopographic variation, limiting the number of elevated microsites for tree establishment and eventual canopy recovery after ash loss. These results suggest that site wetness is a simple and effective predictor of black ash wetland vulnerability to hydrologic regime change. To that end, we assessed the ability of common terrain metrics to predict site wetness, providing a potential tool to target vulnerable areas for active management efforts.

KEYWORDS

evapotranspiration, groundwater exchange, invasive pest, microtopography, specific yield, terrain analysis

1 | INTRODUCTION

Invasive insect pests are increasingly common throughout North America, causing widespread alterations to forest ecosystems (Kenis et al., 2009). One invasive beetle in particular, the emerald ash borer (EAB, *Agrilus planipennis*), has killed tens of millions of ash (*Fraxinus* sp.) trees in the U.S. (USDA, 2019). Of pressing concern is the impending spread of EAB into the western Great Lakes region, where black ash (*Fraxinus nigra*)-dominated wetlands cover over 400,000 ha (MN DNR, 2003). These forested wetlands are often monospecific

stands, with black ash contributing 70–100% of the canopy cover (D'Amato et al., 2018; Palik, Ostry, Venette, & Abdela, 2011). Black ash is considered a foundational species (sensu Ellison et al., 2005) for its role in modulating the structure and function of these ecosystems through influences on hydrology, carbon cycling, and resource availability (Youngquist, Eggert, D'Amato, Palik, & Slesak, 2017).

One of the primary concerns for EAB-induced black ash mortality is a reduction of evapotranspiration (ET), leading to increased water levels during the growing season (Diamond, McLaughlin, Slesak, D'Amato, & Palik, 2018; Slesak, Lenhart, Brooks, D'Amato, & Palik, 2014; Van Grinsven et al., 2017). These wetter conditions may persist for years following tree mortality (Diamond et al., 2018), resulting in an ecohydrologic regime shift to an open-canopy marsh system with associated shifts in ecosystem functions (Kolka et al., 2018; Youngquist et al., 2017). Yet, these observations are largely based on one type of hydrogeomorphic setting and using experimental simulation (via tree girdling) to assess potential impacts of EAB, which has yet to infest black ash wetlands in the region. Vulnerability to hydrologic regime shifts in other hydrogeomorphic settings is largely unknown (Kolka et al., 2018), but is needed to help prioritize active management of black ash wetlands in the western Great Lakes region (D'Amato et al., 2018). In this work, we take an important step in filling this knowledge gap by assessing differences in pre-EAB hydrologic regimes among different black ash hydrogeomorphic settings with predictions on how such regimes may influence vulnerability to EAB-induced mortality.

Hydrogeomorphic setting controls wetland hydrologic regimes (i.e., water flows and levels) via connectivity to surface waters and intersection with regional and local groundwater systems (Carter, 1996; Winter, 1988; Winter, Harvey, Lehn Franke, & Alley, 1998). Three common hydrogeomorphic settings for black ash wetlands in the western Great Lakes region include extensive lowland flats, small isolated depressions surrounded by uplands, and flat linear transition features between uplands and peatlands (MN DNR, 2018). These wetland types are thought to differ in wetness, where lowland sites are generally drier with less inundation compared to depression and transition sites (Diamond, McLaughlin, Slesak, & Stovall, 2019). However, there has been limited quantitative comparisons among hydrogeomorphic settings regarding hydrologic flows and resultant water level regimes, which may lead to site differences in ET response following tree mortality.

Water level (i.e., the elevation of water table relative to ground surface) exerts a primary control on wetland ET rates and partitioning (Rodriguez-Iturbe, D'Odorico, Laio, Ridolfi, & Tamea, 2007). For times when water levels are belowground, water level position influences ET dynamics via its control on water availability for soil evaporation and transpiration (Cooper, Sanderson, Stannard, & Groeneveld, 2006). Under inundated conditions (defined throughout as water level > 0), open water evaporation can become an additional and dominant ET component, often exceeding transpiration rates (Allen, Reba, Edwards, & Keim, 2017). Our previous work in lowland flats suggests that this water level control may determine the extent of ET reduction following tree mortality. That past work simulated EAB-induced mortality via tree girdling and found decreases in growing season ET and water level rises up to 80 cm compared to controls (Diamond et al., 2018; Slesak et al., 2014). However, the largest water level increases occurred during drier conditions (i.e., water levels < −30 cm) because open water/soil water evaporation and shallow-rooted transpiration could compensate for reduced overstory ET in wetter conditions. These ET offsets during higher water levels inform our conceptual model of EAB impacts, where we expect that wetter sites will be less vulnerable to ET reductions and water level increases (Figure 1).

Local bathymetry and surface elevation variation further modulate the spatiotemporal distribution of wetland water levels (Malhotra, Roulet, Wilson, Giroux-Bougard, & Harris, 2016). For example, small depressional wetlands are typically characterized by shallow to deep inundation going from wetland edge to center, whereas larger lowland flats have more spatially uniform water levels across broader areas. Finer scale differences in elevation (i.e., microtopography) further increase spatial variation in water levels, and often manifest as higher (and drier) hummock and lower (wetter) hollow microsites (Nungesser, 2003; Strack, Waddington, Rochefort, & Tuittila, 2006). We therefore distinguish between two perspectives of wetland water level regimes: (1) a *temporal* regime which is typically assessed by measurement of water levels at a point in space (e.g., an observation well), and (2) a *spatial* regime, which is the ensemble of point-scale temporal regimes across a wetland.

Across many wetland systems, microtopographic relief covaries with site wetness due to hydrologic controls on organic matter and soil accumulation (Diamond et al., 2020 and references therein). Our past work further demonstrates this in black ash wetlands: wetlands with higher mean *temporal* water levels exhibit greater microtopographic variation compared to drier sites (Diamond et al., 2019). Consequently, "wetter" sites may exhibit wider *spatial ranges* of water levels, with associated controls on vegetation composition. Indeed, in such wetter sites, black ash trees preferentially occupy hummock locations (Diamond, McLaughlin, Slesak, & Stovall, 2020). These previous observations further inform our conceptual model, where we predict that wetter sites with more hummock features will enable establishment of replacement tree species (D'Amato et al., 2018), potentially mitigating impacts of black ash loss due to EAB (Figure 1). As such, evaluations of hydrologic regime vulnerability to EAB-induced ash mortality would benefit from water level measurements collected over time and space.

Assessments of wetland water level regimes can be infeasible across landscape scales using in-situ measurements, calling for alternative approaches such as terrain-based predictions. With the growing availability of high-spatial resolution elevation data, analysis of wetland landscape position and terrain attributes is increasingly feasible. Numerous studies have used terrain metrics to successfully distinguish wetlands from uplands in many different landscape settings (e.g., Bwangoy, Hansen, Roy, De Grandi, & Justice, 2010; Rampi, Knight, & Pelletier, 2014; Wright & Gallant, 2007). However, terrain metrics can also document wetland differences in bathymetry, relation to surrounding landscapes (e.g., relative elevation and contributing

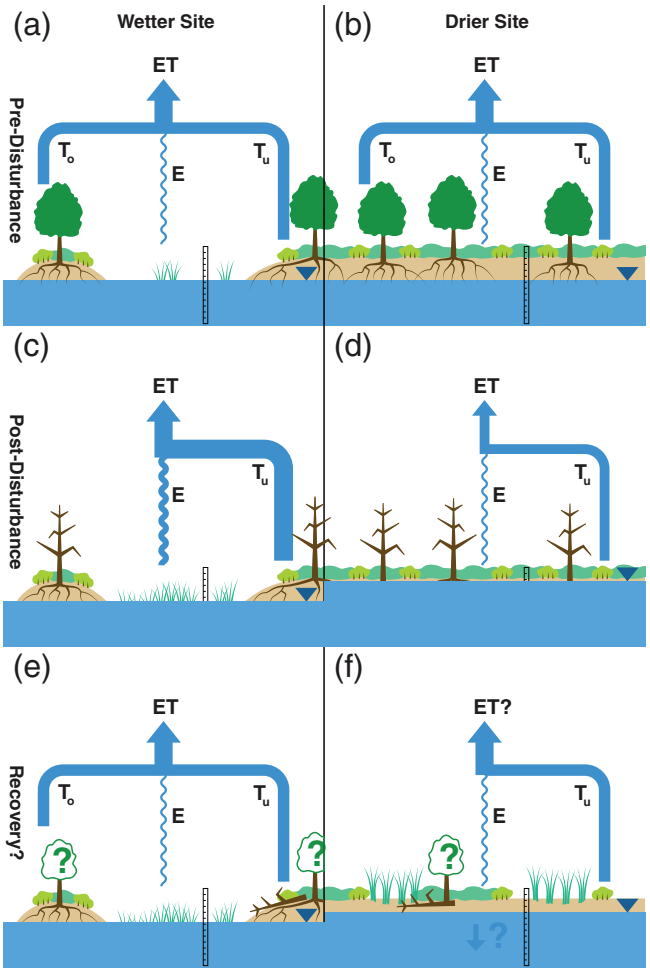

FIGURE 1 Conceptual model of vulnerability to hydrologic regime change from EAB-induced black ash (*Fraxinus nigra*) mortality in black ash wetlands of the western Great Lakes region. Top panel: Pre-infestation conditions in (a) wetter sites and (b) drier sites. Wetter sites likely have greater microtopography and thus variation in point-scale water level. Middle panel: Ecosystem states immediately post-disturbance in (c) wetter sites and (d) drier sites. Ash mortality and loss of overstory transpiration (T_o) occurs in both sites, but we expect that ET will remain similar in wet sites as open water evaporation (E) and understory transpiration (T_u) increase. In contrast, we predict that water levels will increase in panel D because open water evaporation and T_u cannot offset the loss of T_o under drier conditions and less water availability. Bottom panel: Predicted recovery of black ash wetlands post-disturbance in (e) wetter sites and (f) drier sites. We expect that more microtopographic variation in wetter sites (panel e) will help regeneration of replacement overstory species (green outlined trees with question marks), such as swamp white oak (*Quercus bicolor*) and balsam poplar (*Populus balsamifera*). In drier sites, we predict a slow return to pre-disturbance ET driven by higher water levels (i.e., more water availability) and herbaceous vegetation establishment. Fallen ash trees in both system types may provide a form of drier hummock feature where replacement overstory can grow

area), and their integrated controls on water level regimes. Consequently, terrain analysis could prove useful in predicting water level regimes in black ash wetlands across different hydrogeomorphic settings and thus may help managers assess vulnerability to hydrologic regime shifts and the need for active management.

Motivated by our conceptual model (Figure 1), the main goal of our study was to quantify hydrogeomorphic controls on black ash wetland hydrology as a first step in assessing potential site vulnerability. We further sought to evaluate simple, easily accessible terrain metrics as predictors of site water level regime and therefore as potential tools to identify vulnerable areas at regional scales. To do so, we integrated water level and elevation data from 15 undisturbed black ash wetlands in three different hydrogeomorphic settings of northern Minnesota: lowland, depression, and transition sites. We addressed three specific questions: (1) Do sites (and thus hydrogeomorphic settings) vary in *temporal* water level regimes, hydrologic flows (groundwater and ET), and thus potential vulnerability to water level increases following EAB-induced mortality? (2) Do sites vary in *spatial* water level regimes (i.e., microtopography), and thus potential to support replacement tree species following EAB-induced mortality? (3) Can common terrain-based metrics explain differences in site wetness and thus predict vulnerability to hydrologic regime shifts following EAB-induced mortality?

2 | METHODS

2.1 | Site description

We studied 15 non-EAB infested black ash wetlands in Cass, Itasca, and St. Louis counties, MN USA (Figure 2). We categorized each wetland site based on hydrogeomorphic setting as: (1) depression sites ("D", n = 4), characterized by geographically isolated depressions surrounded by uplands; (2) lowland sites ("L", n = 8), characterized by expansive low-relief flats; and (3) transition sites ("T", n = 3), characterized by flat linear features between peatland bogs and uplands. Further, study sites were classified as either wet or very wet ash swamps based on native plant community (NPC) classifications, the habitat typing system used in the study region (MN DNR, 2018; Supplementary Table S1). The lowland setting contained sites in both NPC classifications, whereas depression and transition sites were only classified as very wet.

Study sites were located within the Northern Minnesota Drift and Lake Plains ecological region in northern Minnesota (MN DNR, 1999). The region is described as complex glacial terrain consisting of gentle to undulating topography with relatively nutrient-poor soils developed from loamy and sandy glacial sediments. Black ash wetlands are generally found in flat and low-lying areas that grade into aspen (*Populus* sp.)- or pine (*Pinus* sp.)-dominated upland forests. Study sites had overstory basal areas ranging from 19.8 to 40.0 m^2 ha^{-1}, with black ash as the main overstory contributor (Supplementary Table S1). Site soil profiles were similar and generally characterized as organic histosols with mucky peats underlain by silty clay lacustrine layers (ranging between 50 and 150 cm below surface), with transition and depression sites having deeper organic layers than lowland sites (Soil Survey Staff, 2020). Black ash wetland hydrology is

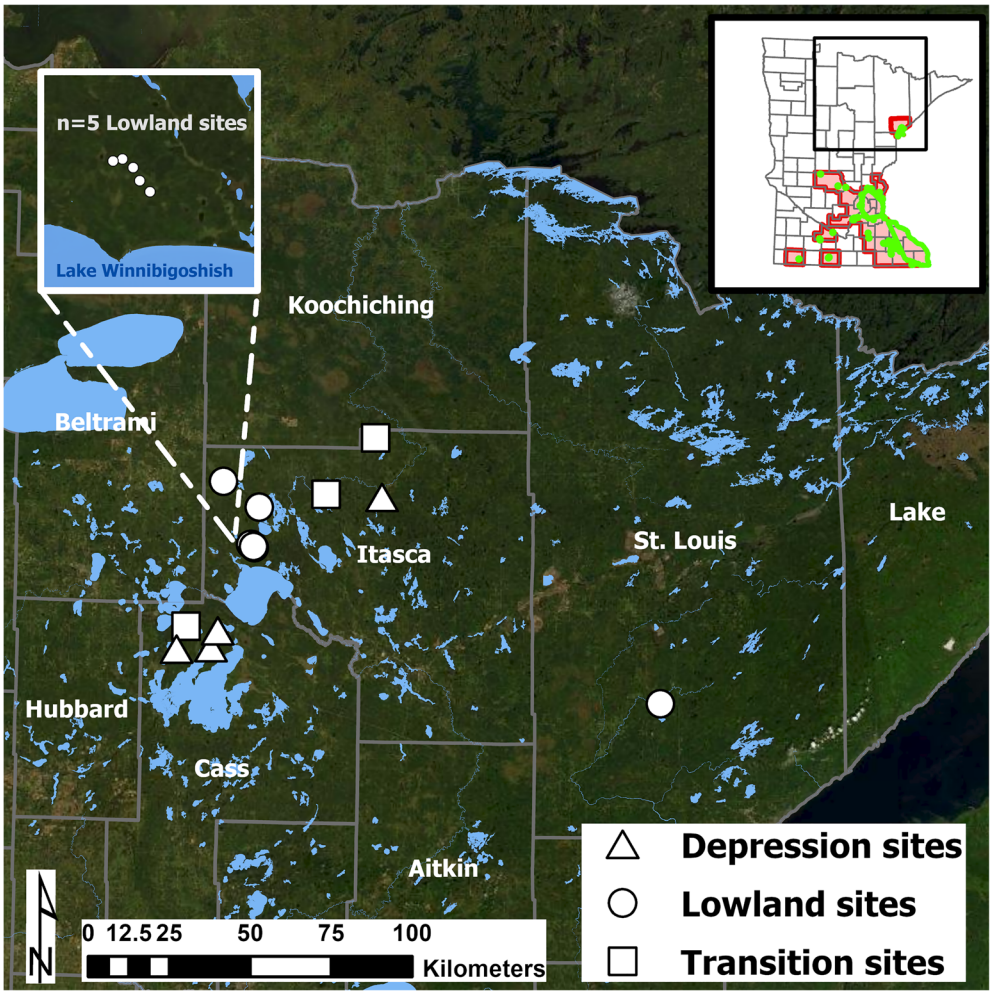

FIGURE 2 Map of 15 black ash (*Fraxinus nigra*) wetland study sites in northern Minnesota. Shape and colour of symbol represent three distinct hydrogeomorphic settings (depression, lowland, and transition). Inset map in the upper right-hand corner shows scale and spread of EAB into Minnesota at the time of publication. Quarantine areas are designated to slow the spread of EAB by restricting movement of ash wood products (e.g., firewood and mulch) to non-quarantine areas. Data can be downloaded from: https://gisdata.mn.gov/dataset/env-emerald-ash-borer

largely driven by local groundwater flowpaths and precipitation, experiencing higher water levels during spring snowmelt followed by general drawdown excepting rainfall events during the growing season (Slesak et al., 2014). Mean annual precipitation is approximately 70 cm, two-thirds of which is snow (Sebestyen et al., 2011). Potential ET (PET) is greatest during the growing season and averages 60 to 65 cm annually (Sebestyen et al., 2011).

2.2 | Data collection

All study sites were monitored for 15-minute water levels from 2016 to 2018 throughout the growing season (May to October, limited otherwise due to frozen conditions) using total pressure transducers (Levelogger Gold Model 3001, Solinst Canada Ltd, Ontario, Canada; and HOBO U20L-04, Onset Computer Corp., Bourne, MA) and atmospheric pressure correction (Barologger, Solinst Canada Ltd, Ontario, Canada). Water level loggers were placed in a 5-cm diameter screened PVC well approximately 1.5 m below the ground surface or when a confining layer was reached. Local rain data were collected at each site with HOBO tipping-bucket rain gauges (model RG3-M, Onset Computer Corp., Bourne, MA). Potential ET data, calculated using the Penman equation, were downloaded from the Cutfoot RAWS station in close proximity to our study sites (https://wrcc.dri.edu/wraws/mnF.html).

To assess spatial water level regimes within sites, we used high-resolution elevation data from previous work characterizing microtopography (see Stovall, Diamond, Slesak, McLaughlin, & Shugart, 2019 for methods). These data are only available for a subset of 10 of our study sites (three lowland sites and all depression and transition sites), where we collected high-resolution LiDAR data using a Faro Focus 120 3D phase-shift terrestrial laser scanner (905 nm λ). Scans were conducted in late October to minimize deciduous leaf cover, grass height, and water inundation. At each site, three random non-overlapping 10 m-diameter plots were scanned to create a $\sim$900 m^2 point cloud. Ten 7.62 cm radius spheres were placed at each site for maximum visibility to facilitate registration of the point cloud. We then created a 1-cm surface elevation model for each site, referencing each site's model to the ground surface of its monitoring well (i.e., elevation = 0).

With these data, we distinguished between two types of water levels: (1) site-scale to assess *temporal* variation at each site, represented by water level data relative to ground surface at the well location (positive indicates inundation), and (2) point-scale to assess *spatial*

variation in water levels within each site, where water level at any particular point is the difference between water level at the well and ground surface elevation at that point (via the 1-cm surface elevation model).

2.3 | Data analysis

2.3.1 | Temporal water level regimes and hydrologic flows

Differences in site-scale daily water levels among hydrogeomorphic settings were assessed using a repeated measures ANOVA analysis on weekly mean values with site and year as random effects. Weekly mean site-scale water levels were left-skewed, so a Tukey's Ladder of Power (Tukey, 1977) was calculated using the *rcompanion* package in R (Mangiafico, 2020) and then applied to the data to produce an approximately normal distribution. The percent of days with flooded conditions and percent of days with daily mean water level below −30 cm were also calculated and compared among settings. The −30 cm metric was selected because previous studies in black ash wetlands have shown that ET reductions and water level increases in stands with EAB-simulated mortality occur largely when water levels are below this threshold (Diamond et al., 2018; Slesak et al., 2014).

Using site-scale water level data, we also calculated daily ET, groundwater fluxes, and water level change to compare differences among hydrogeomorphic settings in hydrologic flows and associated water level responses. Daily ET was calculated using a modified White method (1932) first described by Loheide, Butler, and Gorelick (2005) and used previously at some of our study sites by Diamond et al. (2018). This method allows ET to be calculated from the 24-hr change in water level (S) and rate of groundwater inflow as a function of detrended water level (r) and is corrected for specific yield (S_y). The method is only applied to non-precipitation days and assumes ET is negligible at night:

$$ET = S_y \times [r - S] \tag{1}$$

Specific yield is a dimensionless ratio that, on an area basis, is defined as the water added (e.g., precipitation) or lost (e.g., ET) to storage per unit change in water level [L L^{-1}] (Healy & Cook, 2002). Importantly, in shallow water level environments, S_y varies as a function of both below (Duke, 1972) and aboveground (McLaughlin & Cohen, 2014) water levels. For inundated conditions, S_y approaches unity as water levels increase, but for belowground water levels S_y is much lower (e.g., 0.1–0.3) dependent on both soil type and water level position. This means that for the same ET or rainfall amount, water levels will change much less (e.g., by an order of magnitude) in inundated versus non-inundated conditions. In this study, we calculated site-specific S_y–water level relationships using ratios of rain (corrected for interception) to induced water level rise across a range of water levels (see Diamond et al., 2018; McLaughlin & Cohen, 2014). This calculation assumes negligible infiltration-excess surface runoff, which is reasonable for our sites based on personal observations during rain events.

Groundwater exchange at our study sites is dominated by local, shallow flowpaths as opposed to regional groundwater flows (Slesak et al., 2014) and was calculated using a daily water balance method for wetland flows (McLaughlin, Diamond, Quintero, Heffernan, & Cohen, 2019). While this method generally yields combined surface and subsurface flows into (+) and out of (–) the wetland, here we consider daily rates primarily as shallow subsurface flows because surface flows in our study sites are rare during the growing season (J. Diamond, personal observation). Thus, following McLaughlin et al. (2019), net daily groundwater exchange was estimated based on 24-hr change in water level (S) adjusted for S_y, while accounting for PET and precipitation (P):

$$Groundwater\ exchange = S * S_y - P + PET \tag{2}$$

Differences in ET and groundwater exchange among hydrogeomorphic setting were assessed using a repeated measures ANOVA analysis on weekly mean values with site and year as random effects. Weekly mean ET was positive skewed and Tukey's Ladder of Power (Tukey, 1977) was calculated and then applied to the data to produce an approximately normal distribution. Weekly mean groundwater exchange had negative skewness and high kurtosis, so a Lambert W transformation was applied to the data using the *bestNormalize* package in R (Peterson & Cavanaugh, 2019) to produce an approximately normal distribution.

2.3.2 | Microtopography and spatial water level regimes

For the subset of sites (n = 10) previously assessed for microtopography, we calculated point-scale mean daily water levels at a 1-cm spatial resolution. To do so, we subtracted each point's elevation (via the surface elevation model) from the daily mean site-level water level (at the well location and relative to ground surface = 0 m), while assuming the water level is flat across each study site. We then assessed differences in these spatial water level distributions among hydrogeomorphic categories using one-way ANOVA.

2.3.3 | Terrain-based predictors of site wetness

To explore terrain drivers of hydrology across sites, we used a landscape-scale, high-resolution (1-m) bare earth DEM (https://www.mngeo.state.mn.us/chouse/elevation/lidar.html) with a nominal vertical accuracy root mean square error of approximately 5 cm. Before analysis, the DEM underwent standard cleaning procedures, including filling of sinks less than the vertical accuracy of the DEM and smoothing via a moving-window Gaussian filter to remove random errors (Jones et al., 2018). Ten terrain metrics (Table 1) were calculated using tools freely available in the Whitebox GAT toolbox (Lindsay, 2018)

TABLE 1 Summary table of terrain metrics used as explanatory predictors of mean site-scale water level

Analysis	Description	Citation
Deviation from mean elevation	Difference in elevation between a grid cell and the mean elevation of a user-defined surrounding search window, normalized by standard deviation	Wilson and Gallant, 2000
Ruggedness Index	Local topographic relief calculated as the root mean square deviation of elevation for each cell	Riley, DeGloria, and Elliot, 1999
Height above nearest drainage	Elevation of each grid cell above the nearest stream cell, following downstream flowpaths	Renno et al., 2008
Slope	Slope gradient of each grid cell	Horn, 1981; Wilson and Gallant, 2000
Downslope Index	Measure of slope gradient between a grid cell and a user-defined vertical decline following downstream flow paths	Hjerdt, McDonnell, Seibert, and Rodhe, 2004
Distance Downslope	Distance of each cell to the nearest stream cell following downstream flow paths	Lindsay, 2018
Contributing area	Flow accumulation (upslope area) calculated using the D8 algorithm	O'Callaghan and Mark, 1984
Topographic Wetness index	Measure of wetness incorporating upslope contributing area and slope	Gessler, Moore, McKenzie, and Ryan, 1995; Moore, Gessler, Nielsen, and Petersen, 1993
Plan curvature	Second derivative of topographic surface; curvature perpendicular to slope	Wilson and Gallant, 2000
Profile curvature	Second derivative of topographic surface; curvature parallel to slope	Wilson and Gallant, 2000

with relevant R code available in Supplemental Material. These metrics have been widely used in other studies to identify wetland areas (e.g., Bwangoy et al., 2010; Maxwell, Warner, & Strager, 2016; O'Neil, Goodall, & Watson, 2018; Wright & Gallant, 2007) and include measures of local surface topography (e.g., curvature), relation to downstream drainage networks (e.g., height above nearest drainage), and relative topographic position (e.g., deviation from mean elevation). Here, however, we uniquely used such metrics to characterize different topographic properties of wetlands and their potential influence on water level regimes.

Derived raster layers for each terrain metric were smoothed to remove microtopographic noise not representative of landscape features using a mean filter with a 5 × 5 m window (O'Neil et al., 2018). To obtain a representative site value for each metric, we calculated the mean of all grid cell values within a 30-m diameter buffer centered on each site's well. At some sites, this buffer was adjusted to avoid manmade features (e.g., roads) not representative of site hydrology. We used multiple linear regression to assess the relationship between mean daily site-scale water level and terrain metrics. We then identified the multiple linear regression model with the lowest Bayesian Information Criteria (BIC) value and highest adjusted R^2 using the *Leaps* package in R (Lumley & Miller, 2009). The relative importance of each metric in the best subset model was determined by calculating the R^2 contribution averaged over orderings among regressors for each terrain metric using the "lmg" method (Lindeman, Merenda, & Gold, 1980) from the *relaimpo* package in R (Grömping, 2006).

3 | RESULTS

3.1 | Temporal water level regimes and hydrologic flows

Across all study sites, we observed consistent temporal trends in site-scale water levels (i.e., water level relative to ground surface at well location) described by seasonal drawdowns in late summer (Figure 3a), which were more pronounced at lowland sites, punctuated by rain-induced increases. Repeated measures ANOVA indicated differences in transformed weekly mean site-scale water levels across hydrogeomorphic settings with significant differences (via post-hoc Tukey analysis; p = .002) between lowland and depression sites (Tables 2 and 3). However, differences between transition and depression and lowland sites were negligible (p = .471 and p = .130, respectively). Time had a clear effect on site-scale water levels (i.e., lower water levels during summer months; Figure 3a) across all hydrogeomorphic settings, with no significant interaction between week and hydrogeomorphic setting (Table 3).

Temporal distributions of daily site-scale water levels further illustrate differences among hydrogeomorphic categories, where lowland sites generally experienced drier and more temporally variable water level conditions (Figure 3b). However, there was also variation within hydrogeomorphic setting, particularly for the two wetter lowland sites (L4 and L6) with mean water levels near ground surface, similar to those at depression and transition sites. We also observed differences among hydrogeomorphic settings in percent of daily site-scale water levels below −30 cm and percent time inundated (Table 2). Lowland sites generally spent longer periods of the growing season below −30 cm compared to depression and transition sites. Similarly, lowland sites experienced less time inundated compared to depression and transition sites.

While there were clear differences in site water level regimes, daily ET and groundwater rates were more similar among sites and hydrogeomorphic categories (Table 2). Daily ET rates exhibited a

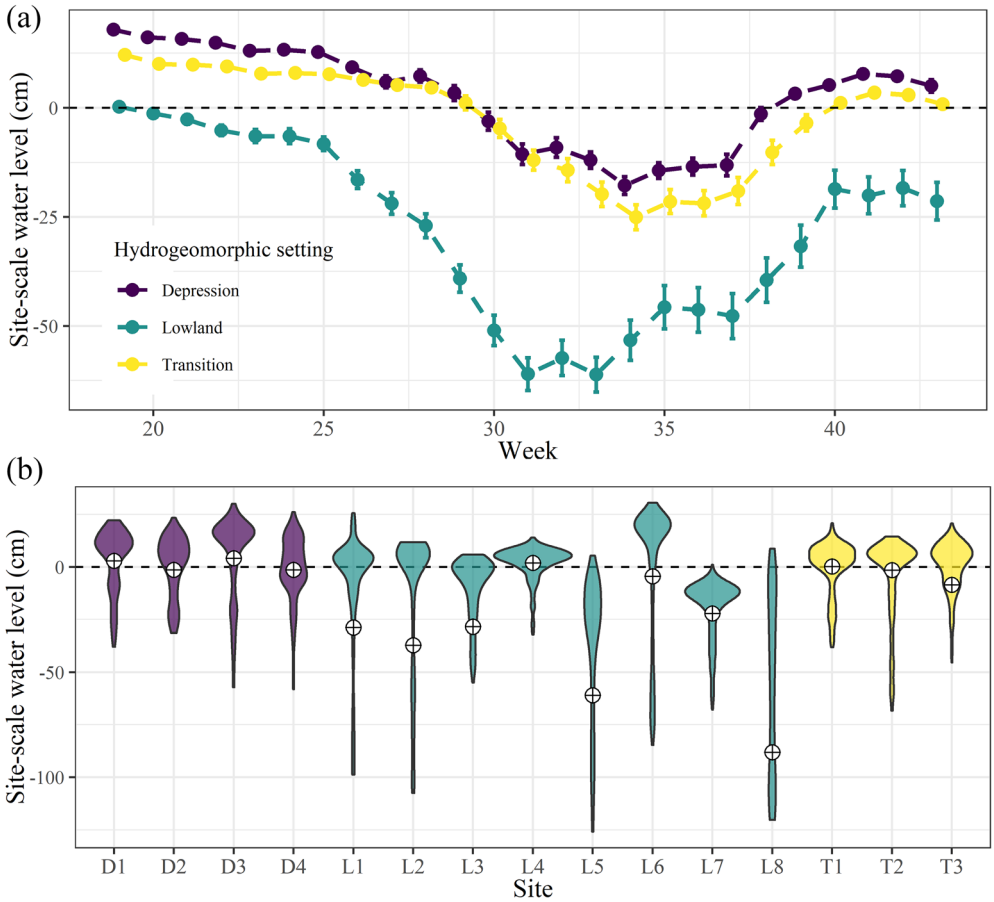

FIGURE 3 (a) Time series of weekly mean site-scale water level grouped by hydrogeomorphic setting with standard error bars. (b) Violin plots that show the temporal distribution and relative frequency of daily site-scale water levels at all study sites. The shoulders of the violin plots are created using a non-parametric kernel density estimation that displays data frequency (i.e., higher frequency equals wider violin plot shoulder). Crossed circles indicate mean daily site-scale water level

TABLE 2 Summary table of mean water level metrics and hydrologic flows ± standard error for each hydrogeomorphic setting

Hydrogeomorphic setting	Weekly mean site-scale water level (cm)	Percent time with water level below −30 cm (%)	Percent time inundated (%)	Weekly mean evapotranspiration (cm d^{-1})	Weekly mean groundwater flow (cm d^{-1})	Variation in point-scale water level (m)
Depression	1.5 ± 1.2	7.9 ± 1.5	67.1 ± 3.6	−0.47 ± 0.02	−0.24 ± 0.01	0.86 ± 0.23
Transition	−2.8 ± 1.4	10.7 ± 5.0	64.2 ± 4.0	−0.33 ± 0.01	−0.16 ± 0.01	1.05 ± 0.10
Lowland	−32.0 ± 2.3	38.5 ± 8.5	32.1 ± 10.4	−0.44 ± 0.02	−0.20 ± 0.02	0.68 ± 0.07

TABLE 3 F-statistics and associated p-values for hydrogeomorphic setting effects on hydrologic parameters

Parameter	Weekly mean site-scale water level		Evapotranspiration		Groundwater flow		Point-scale water level	
Effect	*F*-stat	*p*-Value	*F*-stat	*p*-Value	*F*-stat	*p*-Value	*F*-stat	*p*-Value
Hydrogeomorphic setting	7.1	.002	2.0	.143	2.9	.076	13.4	.004
Week	35.3	<.001	15.0	<.001	9.7	<.001	NA	
Hydrogeomorphic setting*Week	0.8	.777	0.9	.697	2.1	<.001	NA	

seasonal pattern across all hydrogeomorphic settings described by lower rates at the beginning and end of the growing season and higher rates in mid-summer (Supplementary Figure S1A), concordant (although mirrored) with seasonal water level patterns (Figure 3a). Repeated measures ANOVA indicated that transformed weekly mean ET did not differ across hydrogeomorphic setting, and there was no interaction between week and hydrogeomorphic setting (Table 3). However, strong effects were found for week. Local groundwater exchange tended to be lower in the beginning and end of the growing season and higher (as outflow) during the summer (Supplementary Figure S1B). There was a significant interaction between week and hydrogeomorphic setting (Table 3), where groundwater exchange

rates differed across hydrogeomorphic setting for weeks 21, 26, 28, and 39, but there was no consistent pattern in the response.

Despite similar ET and groundwater flows across hydrogeomorphic settings, we observed distinct differences in mean daily water level change (Figure 4), helping to explain site differences in temporal water level regimes. Drier lowland sites had greater mean rates of both water level increases and decreases compared to transition and depression sites via lower S_y. Sites in Figure 4 are ordinated by increasing median daily S_y, where daily S_y values vary with water level position (see Section 2). Low S_y values, which coincide with belowground water levels, induce greater water level response for a given inflow or outflow. Accordingly, we observed that median daily S_y was generally lower in the lowland sites (0.23 ± 0.07 SE), which exhibited greater water level changes, compared to the wetter depression (0.50 ± 0.03 SE) and transition sites (0.41 ± 0.06 SE). We note, however, that the two wetter lowland sites (L4 and L6) experienced similar median S_y values and thus daily water level change as depression and transition sites.

3.2 | Microtopography and spatial water level regimes

For the subset of sites analysed for microtopographic variation, point-scale water levels (i.e., difference between mean water level at the well and local ground surface elevations) documented spatial variation to also consider when comparing water level regimes among sites (see examples in Figure 5). At each site, we note the difference in mean daily water level recorded at the well (i.e., site-scale water levels; crossed circles) compared to the full spatial distribution (Figure 6). One-way ANOVA indicated an effect of hydrogeomorphic setting on point-scale water level distribution with lowland sites having less spatial variation in point-scale water levels compared to transition (p = .050) and depression (p = .003) sites, which themselves did not differ (p = .170) (Tables 2 and 3). Notably, depression and transition sites had many locations with point-scale water levels similar to those at drier lowland sites due to higher and thus drier hummock features (Figures 5b–d and 6).

3.3 | Terrain-based predictors of site wetness

Of the 10 explanatory terrain metrics analysed, deviation from mean elevation (example shown in Supplementary Figure S2) was the only significant individual predictor of mean daily site-scale water level (p = .002; R^2 = 0.54): decreasing values (i.e., lower elevations relative to surrounding areas) increase site-scale water levels (Supplementary Figure S3A and Table S2). Notably, sites L4 and L6 exhibited lower (more negative) values compared to the other lowland sites, coincident with their higher mean water levels. The best subset multiple regression model identified a model with two metrics, deviation from mean elevation and downslope distance (i.e., distance to the nearest stream following downstream flow paths), with the highest adjusted R^2 (0.61) and lowest BIC (Supplementary Figure S3B and Table S3).

4 | DISCUSSION

Ecohydrologic regime shifts from EAB-induced mortality appear imminent for black ash wetlands in the western Great Lakes region;

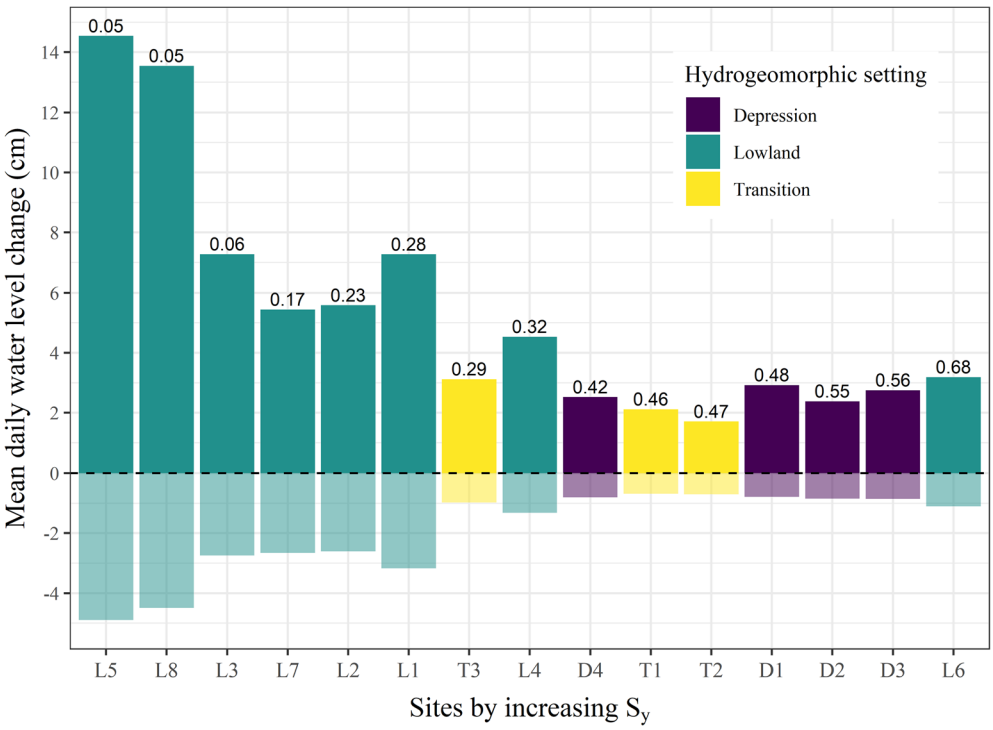

FIGURE 4 Mean increase (top) and decrease (bottom) in daily site-scale water levels for all study sites coloured by hydrogeomorphic setting and ordered by increasing median specific yield (S_y, labelled)

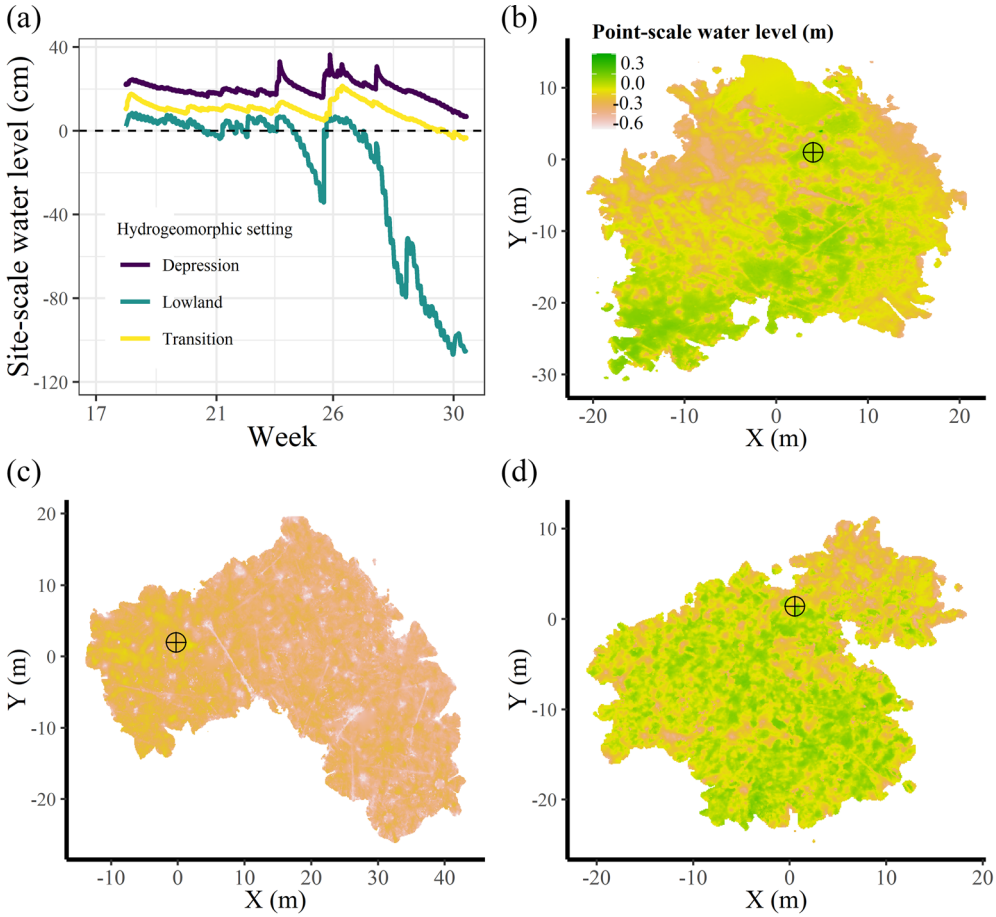

FIGURE 5 (a) Example time series of site-scale water levels relative to well ground surface (dashed line at zero) throughout the growing season from three individual sites representing different hydrogeomorphic settings. For those same three sites, panels (b)–(d) display heat maps of point-scale mean daily water levels (i.e., relative to local ground surface where positive values indicate inundated conditions) within each site (B = depression; C = lowland; and D = transition). Crossed circles in (b)–(d) represent each site's monitoring well location and thus the location of site-scale daily water levels shown in a. the fine-scale topographic and resultant spatial water level variation are clear, including circular hummock features, particularly in the depression (b) and transition (d) sites, and linear features likely representing downed trees

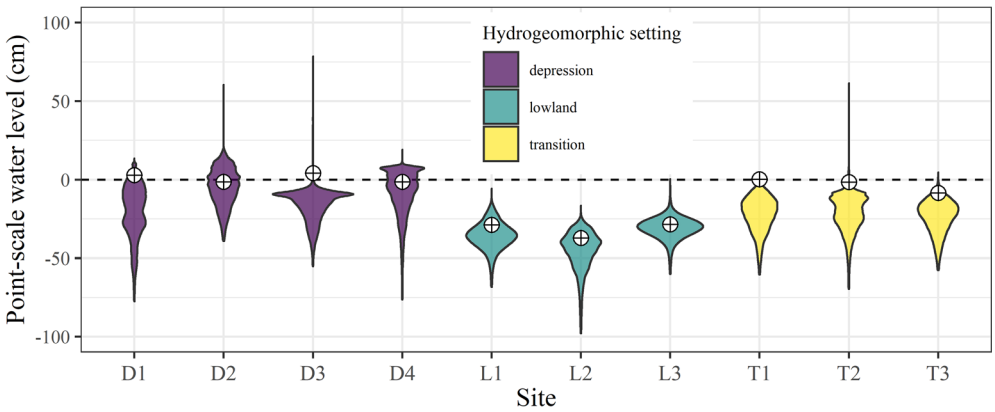

FIGURE 6 Violin plots showing the spatial distribution and relative frequency of point-scale daily mean water levels at a subset of study sites. The shoulders of the violin plots are created using a non-parametric kernel density estimation that displays data frequency (i.e., higher frequency equals wider violin plot shoulder). Crossed circles represent site-scale mean daily water levels measured at the well location (i.e., same crossed circles in Figure 3b)

assessing relative site vulnerability to these shifts is important to inform active management efforts. Motivated by our conceptual model of hydrologic vulnerability to EAB-induced mortality (Figure 1), we evaluated temporal water level regimes and hydrologic flows (Question 1), spatial variation in water level regimes (Question 2), and terrain-based predictions of site wetness (Question 3). Below we discuss these findings and their potential implications for hydrologic vulnerability of black ash wetlands to impending EAB-infestation.

4.1 | Temporal water level regimes and hydrologic flows

Across all hydrogeomorphic settings, site-scale water levels exhibited a consistent seasonal pattern of springtime inundation followed by ET-induced drawdown, but lowland sites generally experienced the greatest drawdown and lowest water levels, particularly in summer months (Figure 3). These differences in water level regimes, however,

were not explained by ET and groundwater exchange rates, which were similar across all sites (Supplementary Figure S1). In contrast, mean daily S_y values varied substantially across sites, resulting in very different responses to similar hydrologic flows (Figure 4). Indeed, daily water levels at the driest lowland sites varied five times more than wetter depression sites, concordant with lower S_y for belowground water levels compared to inundated conditions (McLaughlin & Cohen, 2014). Critically then, as hydrologic inputs and outputs did not vary across settings, initial water level conditions during growing season onset and their effect on S_y appear to be the primary determinants of site hydrology. We note, however, that the two wetter lowland sites (L4 and L6) experienced S_y values and concordant water level responses similar to those of typically wetter depression and transition sites (Figure 4), indicating variability within hydrogeomorphic setting. We suggest that this site variation in S_y values, with reciprocal effects on water level regimes, is largely driven by wetland elevation relative to shallow groundwater.

Together with our conceptual model (Figure 1), observed differences in site-scale water level regimes suggest variation in hydrologic vulnerability to EAB-induced tree mortality among and within hydrogeomorphic settings. As the dominant overstory tree species, black ash transpiration contributes anywhere from 20% to 60% of wetland ET, indicating that understory transpiration and soil/open water evaporation can contribute up to 80% (Telander et al., 2015). However, this contribution decreases under drier conditions (Lafleur, Hember, Admiral, & Roulet, 2005), when black ash is likely the main contributor to ET due to deeper roots for water access. We conclude then that drier lowland wetlands that spend more time with water levels below −30 cm (Diamond et al., 2018; Table 2) are likely more vulnerable to ET reductions and thus water level increases from ash mortality compared to wetter sites (Figure 1c and d).

4.2 | Microtopography and spatial water level regimes

Microtopography creates a spatial range of water levels within a given wetland, highlighting the value of fine-scale bathymetric data coupled to temporal water level analysis. For example, while depression and transition sites had higher site-scale water levels compared to lowland sites, they also had greater microtopographic variability and, consequently, greater point-scale water level variability (Figures 5b–d and 6). Importantly, hummocks in these wetter sites exhibited point-scale water levels similar to site-scale water levels of drier lowland sites. In sites with such microtopographic relief, water level dynamics solely inferred by well data are thus not representative of the spatial suite of regimes experienced by vegetation (Rodriguez-Iturbe et al., 2007). Indeed, black ash trees, and most understory plant species, in wetter sites preferentially occupy drier hummocks with limited vegetation in wetter hollow locations (Diamond, McLaughlin, et al., 2020). Likely a result of biota-hydrology feedbacks, it is at these wetter sites where microtopographic relief is greatest, with high correspondence between site mean water level and hummock height (R^2 = 0.8; Diamond et al., 2019). Hence, mean site-scale water level may be a useful predictor of point-scale water level variability, and consequently, a useful predictor of hydrological niche space for vegetation communities. We note, however, that microtopographic surveys were not conducted at the two wetter lowland sites (L4 and L6). These sites experienced site-scale water levels similar to depression and transition sites, but it remains unknown if they exhibit similar microtopographic variation, which we predict covaries with overall site wetness.

Our conceptual model of hydrologic vulnerability to ash mortality also predicts that greater microtopography will better support colonization of replacement tree species (Figure 1). Many studies have documented that wetland microtopography is important to vegetation recovery following disturbance events (e.g., Moser, Ahn, & Noe, 2007; Alsfield, Bowman, & Deller-Jacobs, 2009; Rossell, Moorhead, Alvarado, & Warren, 2009). In drier sites with fewer and shorter hummocks (Diamond et al., 2019), post-disturbance water level rises may result in spatially uniform hydrologic regimes more similar to the hollow locations of wetter sites where tree occurrence is low (Figure 1c and d). In contrast, we expect that wetter sites with greater microtopographic variation may allow for replacement overstory species on hummock features (Figure 1e and f), with possible species including American elm (*Ulmus americana*), swamp white oak (*Quercus bicolor*), balsam poplar (*Populus balsamifera*), and silver maple (*Acer saccharinum*) (Kolka et al., 2018). In short, we predict that drier lowland settings will be more susceptible to water level increases and also less resilient to those increases (i.e., less microtopographic variation for tree regeneration), together resulting in increased vulnerability to ecohydrologic regime shifts.

4.3 | Terrain-based predictions to inform management

With the impending spread of EAB, management strategies to increase non-ash overstory species are being considered (D'Amato et al., 2018), with the goal of maintaining hydrologic regimes and associated ecosystem benefits for forest structure, wildlife habitat, and carbon cycling and storage (Youngquist et al., 2017). For example, preemptive group selection (i.e., partial harvests) with planting is a promising method of active management where black ash wetlands can be slowly transitioned to other facultative wetland tree species (D'Amato et al., 2018), without a dramatic shift in hydrologic regime (Diamond et al., 2018). Further, the creation of microtopography (e.g., leaving cut ash trees on the ground surface) in active management areas could facilitate the development of hummock features where non-ash trees could begin to grow despite increasing water levels (Figure 1f). However, black ash wetlands across all hydrogeomorphic settings cover vast tracts of land in the western Great Lakes region, accounting for 400 000 ha in Minnesota alone (MN DNR, 2003). Consequently, active management may be limited to small, targeted areas, highlighting the importance of predictive tools that can identify areas most vulnerable to hydrologic regime shifts.

Our conceptual model posits that drier sites are more vulnerable to a change in hydrologic regime than wetter sites, highlighting the potential for predictions of site wetness to inform targeted management efforts. Site differences in water level regimes are likely driven by differences in wetland elevation relative to shallow groundwater, which may be well-represented by the deviation from mean elevation terrain metric. In support, this metric was the strongest predictor of site wetness and, importantly, helped to distinguish the two wetter lowland sites (L4 and L6; Supplementary Figure S3) from the other lowland sites, consistent with their differences in water level regimes (Figure 4). As such, simple, landscape-level topographic assessment of black ash wetlands as opposed to hydrogeomorphic and NPC categorical characterizations may more effectively indicate water level regimes and potential vulnerability. As more detailed maps of black ash presence become available (e.g., Host, Russell, Windmuller-Campione, Slesak, & Knight, 2020), such terrain metrics could be used to determine the most vulnerable areas to ecohydrologic regime shift from EAB.

4.4 | Future work

This study is an important step in understanding how sites may vary in their vulnerability to a change in hydrologic regime following EAB-induced ash mortality. However, our focus was to characterize site differences in pre-EAB hydrologic regimes (i.e., temporal and spatial water levels) following the expectation that wetter sites with more microtopography are less vulnerable. While this prediction is supported by work in black ash wetlands and wetland systems more broadly, future work would be needed to test our conceptual model. To do so will require studies of either EAB-simulations (as already done in lowland systems) or assessment of post-EAB conditions across different hydrogeomorphic settings, with focus on ET rates and partitioning, water level rise, and tree regeneration dynamics. Yet, EAB invasion is imminent, and such research requires extensive resources and timelines. Thus, we suggest that findings here and terrain-based predictions of site wetness provide an opportunity to develop predictive tools for targeting vulnerable areas. These could be further coupled to forest community mapping and process models to identify regions where intervention (cf. group-selection and planting) can be most efficient at sustaining processes and functions associated with black ash wetlands.

ACKNOWLEDGEMENTS

This project was funded by the Minnesota Environmental and Natural Resources Trust Fund, the USDA Forest Service Northern Research Station, the Minnesota Forest Resources Council, and the Department of Interior Northeast Climate Adaptation Science Center. We gratefully acknowledge the logistic support of staff from the Chippewa National Forest, the field work and data collection assistance provided by Mitch Slater and Josh Kragthorpe, digital elevation model acquisition from Jennifer Corcoran, and assistance developing terrain analysis code by Nate Jones.

DATA AVAILABILITY STATEMENT

The data that support the findings of this study are available from the corresponding author upon reasonable request.

ORCID

Thomas R. Cianciolo https://orcid.org/0000-0003-3051-7687
Jacob S. Diamond https://orcid.org/0000-0002-5392-5707
Daniel L. McLaughlin https://orcid.org/0000-0001-7394-4780
Brian J. Palik https://orcid.org/0000-0003-0300-9644

REFERENCES

Allen, S. T., Reba, M. L., Edwards, B. L., & Keim, R. F. (2017). Evaporation and the subcanopy energy environment in a flooded forest. *Hydrological Processes*, *31*(16), 2860–2871.

Alsfeld, A. J., Bowman, J. L., & Deller-Jacobs, A. (2009). Effects of woody debris, microtopography, and organic matter amendments on the biotic community of constructed depressional wetlands. *Biological Conservation*, *142*(2), 247–255. https://doi.org/10.1016/j.biocon.2008.10.017.

Bwangoy, J. R. B., Hansen, M. C., Roy, D. P., De Grandi, G., & Justice, C. O. (2010). Wetland mapping in The Congo Basin using optical and radar remotely sensed data and derived topographical indices. *Remote Sensing of Environment*, *114*(1), 73–86. https://doi.org/10.1016/j.rse.2009.08.004.

Carter, V. (1996). Wetland hydrology, water quality, and associated functions. In *National Water Summary on Wetland Resources* (pp. 35–48). Reston, Virginia: United States Geological Survey.

Cooper, D. J., Sanderson, J. S., Stannard, D. I., & Groeneveld, D. P. (2006). Effects of long-term water table drawdown on evapotranspiration and vegetation in an arid region phreatophyte community. *Journal of Hydrology*, *325*(1–4), 21–34.

D'Amato, A. W., Palik, B. J., Slesak, R. A., Edge, G., Matula, C., & Bronson, D. R. (2018). Evaluating adaptive management options for black ash forests in the face of emerald ash borer invasion. *Forests*, *9*(6), 348.

Diamond, J. S., Epstein, J. M., Cohen, M. J., McLaughlin, D. L., Hsueh, Y., Keim, R. F., & Duberstein, J. A. (2020). A little relief: Ecological functions and autogenesis of wetland microtopography. *WIREs Water*. *8*(1), e1493. https://doi.org/10.1002/wat2.1493.

Diamond, J. S., McLaughlin, D. L., Slesak, R. A., D'Amato, A. W., & Palik, B. J. (2018). Forested versus herbaceous wetlands: Can management mitigate ecohydrologic regime shifts from invasive emerald ash borer? *Journal of Environmental Management*, *222*, 436–446.

Diamond, J. S., McLaughlin, D. L., Slesak, R. A., & Stovall, A. (2019). Pattern and structure of microtopography implies autogenic origins in forested wetlands. *Hydrology and Earth System Sciences*, *23*, 5069–5088. https://doi.org/10.5194/hess-23-5069-2019.

Diamond, J. S., McLaughlin, D. L., Slesak, R. A., & Stovall, A. (2020). Microtopography is a fundamental organizing structure of vegetation and soil chemistry in black ash wetlands. *Biogeosciences*, *17*, 901–915. https://doi.org/10.5194/bg-17-901-2020.

Duke, H. R. (1972). Capillary properties of soils-influence upon specific yield. *Transactions of the ASAE*, *15*(4), 688–691.

Ellison, A. M., Bank, M. S, Clinton, B. D., Colburn, E. A., Elliott, K., Ford, C. R., Foster, D. R., … Webster, J. R. (2005). Loss of foundation species: Consequences for the structure and dynamics of forested ecosystems. *Frontiers in Ecology and the Environment*, *3*(9), 479–486.

Gessler, P. E., Moore, I. D., McKenzie, N. J., & Ryan, P. J. (1995). Soil-landscape modelling and spatial prediction of soil attributes. *International Journal of Geographic Information Systems*, *9*(4), 421–432.

Grömping, U. (2006). Relative importance for linear regression in R: The package relaimpo. *Journal of Statistical Software*, *17*, 1–27. https://doi.org/10.1360/jos170001.

Healy, R. W., & Cook, P. G. (2002). Using groundwater levels to estimate recharge. *Hydrogeology Journal*, *10*(1), 91–109.

Hjerdt, K. N., McDonnell, J. J., Seibert, J., & Rodhe, A. (2004). A new topographic index to quantify downslope controls on local drainage. *Water Resources Research*, *40*, W05602. https://doi.org/10.1029/2004WR003130.

Horn, B. K. (1981). Hill shading and the reflectance map. *Proceedings of the IEEE*, *69*(1), 14–47.

Host, T. K., Russell, M. B., Windmuller-Campione, M. A., Slesak, R. A., & Knight, J. F. (2020). Ash presence and abundance derived from composite Landsat and Sentinel-2 time series and Lidar surface models in Minnesota, USA. *Remote Sensing*, *12*, 1341. https://doi.org/10.3390/rs12081341.

Jones, C. N., Evenson, G. R., McLaughlin, D. L., Vanderhoof, M. K., Lang, M. W., McCarty, G. W., … Alexander, L. C. (2018). Estimating restorable wetland water storage at landscape scales. *Hydrological Processes*, *32*(2), 305–313.

Kenis, M., Auger-Rozenberg, M. A., Roques, A., Timms, L., Péré, C., Cock, M. J., … Lopez-Vaamonde, C. (2009). Ecological effects of invasive alien insects. *Biological Invasions*, *11*(1), 21–45. https://doi.org/10.1007/s10530-008-9318-y.

Kolka, R. K., D'Amato, A. W., Wagenbrenner, J. W., Slesak, R. A., Pypker, T. G., Youngquist, M. B., … Palik, B. J. (2018). Review of ecosystem level impacts of emerald ash borer on black ash wetlands: What does the future hold? *Forests*, *9*(4), 179. https://doi.org/10.3390/f9040179.

Lafleur, P. M., Hember, R. A., Admiral, S. W., & Roulet, N. T. (2005). Annual and seasonal variability in evapotranspiration and water table at a shrub-covered bog in southern Ontario, Canada. *Hydrological Processes*, *19*(18), 3533–3550.

Lindeman, R., Merenda, P., & Gold, R. (1980). *Introduction to bivariate and multivariate analysis*. Glenview, Il: Scott, Foresman.

Lindsay, J. B. (2018). *WhiteboxTools user manual. Geomorphometry and Hydrogeomatics Research Group*. Guelph, Canada: University of Guelph. Available online: https://jblindsay.github.io/wbt_book/.

Loheide, S. P., Butler, J. J., Jr & Gorelick, S. M. (2005). Estimation of groundwater consumption by phreatophytes using diurnal water table fluctuations: A saturated-unsaturated flow assessment. *Water Resources Research*, *41*(7), W07030. http://dx.doi.org/10.1029/2005wr003942.

Lumley, T., & Miller, A. (2009). Leaps: Regression subset selection. *R package version*, *2*, 2366.

Malhotra, A., Roulet, N. T., Wilson, P., Giroux-Bougard, X., & Harris, L. I. (2016). Ecohydrological feedbacks in peatlands: An empirical test of the relationship among vegetation, microtopography and water table. *Ecohydrology*, *9*(7), 1346–1357.

Mangiafico, S. (2020). *Rcompanion: Functions to support extension education program evaluation. R package version 2.3.25*. https://CRAN.R-project.org/package=rcompanion

Maxwell, A. E., Warner, T. A., & Strager, M. P. (2016). Predicting palustrine wetland probability using random forest machine learning and digital elevation data-derived terrain variables. *Photogrammetric Engineering & Remote Sensing*, *82*(6), 437–447. https://doi.org/10.14358/PERS.82.6.437.

McLaughlin, D. L., & Cohen, M. J. (2014). Ecosystem specific yield for estimating evapotranspiration and groundwater exchange from diel surface water variation. *Hydrological Process*, *28*(3), 1495–1506.

McLaughlin, D. L., Diamond, J. S., Quintero, C., Heffernan, J., & Cohen, M. J. (2019). Wetland connectivity thresholds and flow dynamics from stage measurements. *Water Resources Research*, *55*(7), 6018–6032.

Minnesota Department of Natural Resources (MN DNR). (1999). *Ecological classification system*. Grand Rapids, MN: Division of Forestry, MN DNR. Available online: https://files.dnr.state.mn.us/natural_resources/ecs/section.pdf.

Minnesota Department of Natural Resources (MN DNR). (2003). *Field Guide to the Native Plant Communities of Minnesota: The Laurentian Mixed Forest Province*. St. Paul, MN: Ecological Land Classification Program, Minnesota County Biological Survey, and Natural Heritage and Nongame Research Program. MN DNR.

Minnesota Department of Natural Resources (MN DNR). (2018). *Native Plant Communities for Northern Very Wet Ash Swamp*. Minnesota: MN DNR. Available online: http://files.dnr.state.mn.us/natural_resources/npc/wet_forest/wfn64.pdf (Accessed 08 April 2020).

Moore, I. D., Gessler, P. E., Nielsen, G. Z., & Petersen, G. A. (1993). Terrain attributes: Estimation methods and scale effects. In A. J. Jakeman, M. B. Beck, & M. McAleer (Eds.), *Modeling change in environmental systems* (p. 189). London, United Kingdom, 214: Wiley.

Moser, K., Ahn, C., & Noe, G. (2007). Characterization of microtopography and its influence on vegetation patterns in created wetlands. *Wetlands*, *27*(4), 1081–1097.

Nungesser, M. K. (2003). Modelling microtopography in boreal peatlands: Hummocks and hollows. *Ecological Modelling*, *165*, 175–207.

O'Callaghan, J. F., & Mark, D. M. (1984). The extraction of drainage networks from digital elevation data. *Computer Vision, Graphics, and Image Processing*, *27*(2), 247. https://doi.org/10.1016/S0734-189x(84)80011-0.

O'Neil, G. L., Goodall, J. L., & Watson, L. T. (2018). Evaluating the potential for site-specific modification of LiDAR DEM derivatives to improve environmental planning-scale wetland identification using random Forest classification. *Journal of Hydrology*, *559*, 192–208.

Palik, B. J., Ostry, M. E., Venette, R. C., & Abdela, E. (2011). *Fraxinus nigra* (black ash) dieback in Minnesota: Regional variation and potential contributing factors. *Forest Ecology and Management*, *261*(1), 128–135.

Peterson, R. A., & Cavanaugh, J. E. (2019). Ordered quantile normalization: A semiparametric transformation built for the cross-validation era. *Journal of Applied Statistics*, *47*(13-15), 2312–2327. https://doi.org/10.1080/02664763.2019.1630372.

Rampi, L. P., Knight, J. F., & Pelletier, K. C. (2014). Wetland mapping in the upper Midwest United States. *Photogrammetric Engineering & Remote Sensing*, *80*(5), 439–448. https://doi.org/10.14358/PERS.80.5.439.

Renno, C. D., Nobre, A. D., Cuartas, L. A., Soares, J. V., Hodnett, M. G., Tomasella, J., & Waterloo, M. J. (2008). HAND, a new terrain descriptor using SRTM-DEM: Mapping terra-firme rainforest environments in Amazonia. *Remote Sensing of Environment*, *112*(9), 3469–3481.

Riley, S. J., DeGloria, S. D., & Elliot, R. (1999). Index that quantifies topographic heterogeneity. *Intermountain Journal of Sciences*, *5*(1–4), 23–27.

Rodriguez-Iturbe, I., D'Odorico, P., Laio, F., Ridolfi, L., & Tamea, S. (2007). Challenges in humid land ecohydrology: Interactions of water table and unsaturated zone with climate, soil, and vegetation. *Water Resources Research*, *43*(9), W09301.

Rossell, I. M., Moorhead, K. K., Alvarado, H., & Warren, R. J. (2009). Succession of a southern Appalachian mountain wetland six years following hydrologic and microtopographic restoration. *Restoration Ecology*, *17*(2), 205–214.

Sebestyen, S. D., Dorrance, C., Olson, D. M., Verry, E. S., Kolka, R. K., Elling, A. E., & Kyllander, R. (2011). Chapter 2. Long-term monitoring sites and trends at the Marcell experimental Forest. In R. K. Kolka, S. D. Sebestyen, E. S. Verry, & K. N. Brooks (Eds.), *Peatland biogeochemistry and watershed hydrology at the Marcell experimental Forest* (pp. 15–71). Boca Raton, FL: CRC Press.

Slesak, R. A., Lenhart, C. F., Brooks, K. N., D'Amato, A. W., & Palik, B. J. (2014). Water table response to harvesting and simulated emerald ash borer mortality in black ash wetlands in Minnesota, USA. *Canadian Journal of Forest Research*, *44*(8), 961–968.

Soil Survey Staff. (2020). Natural Resources Conservation Service, United States Department of Agriculture, web soil survey, Available at: https://websoilsurvey.sc.egov.usda.gov/.

Stovall, A. E., Diamond, J. S., Slesak, R. A., McLaughlin, D. L., & Shugart, H. (2019). Quantifying wetland microtopography with terrestrial laser scanning. *Remote Sensing of Environment*, *232*, 111271. https://doi.org/10.1016/j.rse.2019.111271.

Strack, M., Waddington, J. M., Rochefort, L., & Tuittila, E. S. (2006). Response of vegetation and net ecosystem carbon dioxide exchange at different peatland microforms following water table drawdown. *Journal of Geophysical Research: Biogeosciences*, *111*(G2), G2006.

Telander, A. C., Slesak, R. A., D'Amato, A. W., Palik, B. J., Brooks, K. N., & Lenhart, C. F. (2015). Sap flow of black ash in wetland forests of northern Minnesota, USA: Hydrologic implications of tree mortality due to emerald ash borer. *Agricultural and Forest Meteorology*, *206*, 4–11.

Tukey, J. W. (1977). *Exploratory data analysis*. Massachusetts: Addison-Wesley.

USDA Animal and Plant Health Inspection Service. 2019. Emerald ash borer. Available from https://www.aphis.usda.gov/aphis/ourfocus/planthealth/plant-pest-and-disease-programs/pests-and-diseases/emerald-ash-borer

Van Grinsven, M. J., Shannon, J. P., Davis, J. C., Bolton, N. W., Wagenbrenner, J. W., Kolka, R. K., & Pypker, T. G. (2017). Source water contributions and hydrologic responses to simulated emerald ash borer infestations in depressional black ash wetlands. *Ecohydrology*, *10*(7), e1862. https://doi.org/10.1002/eco.1862.

Wilson, J. P., & Gallant, J. C. (2000). *Terrain analysis principles and applications*. Ottawa, ON, Canada: John Wiley and Sons, Inc.

Winter, T. C. (1988). A conceptual framework for assessing cumulative impacts on the hydrology of nontidal wetlands. *Environmental Management*, *12*(5), 605–620.

Winter, T. C., Harvey, J. W., Lehn Franke, O., & Alley, W. M. (1998). *Ground water and surface water: A single resource*. Denver: US Geological Survey.

Wright, C., & Gallant, A. (2007). Improved wetland remote sensing in Yellowstone National Park using classification trees to combine TM imagery and ancillary environmental data. *Remote Sensing of Environment*, *107*(4), 587–605.

Youngquist, M. B., Eggert, S. L., D'Amato, A. W., Palik, B. J., & Slesak, R. A. (2017). Potential effects of foundation species loss on wetland communities: A case study of black ash wetlands threatened by emerald ash borer. *Wetlands*, *37*(4), 787–799. https://doi.org/10.1007/s13157-017-0908-2.

SUPPORTING INFORMATION

Additional supporting information may be found online in the Supporting Information section at the end of this article.

How to cite this article: Cianciolo TR, Diamond JS, McLaughlin DL, Slesak RA, D'Amato AW, Palik BJ. Hydrologic variability in black ash wetlands: Implications for vulnerability to emerald ash borer. *Hydrological Processes*. 2021;35:e14014. https://doi.org/10.1002/hyp.14014